

SOME ASPECTS CONCERNING A NEW POSSIBILITY OF Al-SiC_P COMPOSITE PRODUCTION

Muna N. ISMAEL¹, Hazim F. AL-DULAIMI², Mihai CHISAMERA³, Gigel NEAGU⁴, Florin STEFĂNESCU⁵, Eduard Marius STEFAN⁶

The paper presents the calculations regarding the acceleration and the shape factors for aluminum and aluminum alloy-silicon carbide particle composites. At the same time, due to poor wettability between the silicon carbide and aluminum melt, a new method that uses gravity casting for Al-SiC_P sieves is presented. Different mesh numbers of sieves made from bonded textile fibers and silicon carbide powder were used. Finally, a microscope analysis was carried out for all samples.

Keywords: Aluminum, silicon carbide particles, critical acceleration, shape coefficient, sieves

1. Introduction

Metal matrix composites have been developed and applied as structural materials in the aerospace and automobile industry for many decades due to their high specific strength, high specific stiffness, good high-temperature properties and better wear resistance [1].

Particle reinforced metal matrix composites are now being produced commercially, the different types of reinforcement being used together with alternative processing methods [2]. Aluminum is one of the most desirable metals owing to its desirable properties of corrosion resistance, density ($\rho=2700 \text{ kg/m}^3$), Young modulus (70,000 MPa), tensile strength (90 MPa), and thermal expansion coefficient ($23.5 \cdot 10^{-6} /^\circ\text{C}$) [3]. Silicon carbide is a covalent material of great technological interest due to its excellent overall properties including low density ($\rho=3.1 \dots 3.21 \text{ g/cm}^3$), stability at high temperatures, high hardness (9.2...9.3 on the Mohs' scale), and high value for the modulus of elasticity ($E = 400,000 \text{ MPa}$), low thermal expansion coefficient ($\alpha_{\text{SiC}}=4 \cdot 10^{-6} /^\circ\text{C}$) [4-9].

¹ PhD student, Technical Institute Anbar, Middle Technical University, Iraq, e-mail: muna_alanni2008@yahoo.com

² PhD student, Technical Institute Anbar, Middle Technical University, Iraq

³ Prof., Faculty of Materials Science and Engineering, University POLITEHNICA of Bucharest

⁴ Prof., Faculty of Materials Science and Engineering, University POLITEHNICA of Bucharest

⁵ Prof., Faculty of Materials Science and Engineering, University POLITEHNICA of Bucharest

⁶ PhD student, Faculty of Materials Science and Engineering, University POLITEHNICA of Bucharest, Romania

Aluminum-silicon carbide combines the benefits of high thermal conductivity of metal and low coefficient of thermal expansion of ceramic, possessing high modulus, strength values, wear resistance, high thermal stability, low weight and a more effective load carrying capacity compared to many other materials [10].

The main methods of producing aluminum metal matrix composites are: stir casting, squeeze casting, rheocasting (compo casting), and spray deposition [11-12].

2. Theoretical consideration

Although gravitational casting seems to be the simplest and cheapest method to produce aluminium-silicon carbide particles, a major problem arises concerning the achievement of the mixture by mechanical stirring due to the non-wetting conditions in the system [13, 14]. To penetrate the aluminium melt, a silicon carbide particle needs to exceed a critical acceleration [13]. For a spherical particle, the critical acceleration value can be determined by the relationship:

$$a_{cr} = -\frac{3}{2} \frac{\sigma_{lg}}{r_p^2(\rho_p - \rho_l)} \cdot \cos \theta \quad (1)$$

where: σ_{lg} σ_{lg} is the surface tension at the aluminium melt-gas interface, $\cos \theta$ - the wetting degree, r_p r_p - the radius of the particle, ρ_p - the particle density; ρ_l - the density of the liquid aluminium.

For a spherical particle, equation (1) becomes:

$$r_p = \left[\frac{3m_p}{4\pi\rho_p} \right]^{\frac{1}{3}} \quad (2)$$

$$a_{cr} = k_v \left[\frac{\rho_p}{m_p} \right]^{\frac{1}{3}} \frac{\sigma_{lg} \cos \theta}{\rho_l - \rho_p} \quad (3)$$

where: k_v is a volumetric coefficient of shape, m_p - the particle mass.

For a spherical particle $k_v = 3.896$.

The calculated values of the volumetric coefficient shape for different types of particles are presented in Table 1.

Table 1
Calculated values of volumetric coefficient shape

Shape of particles	Mathematical formula of K_v	Value of K_v
Sphere, $r = r_p$	$(6\pi^2)^{\frac{1}{3}}$	3.896
Cylinder, $r = r_p$, $h = 2r_p$	$3 \left[\frac{\pi^2}{2} \right]^{\frac{1}{3}}$	5.106
Conical, $r = r_p$, $h = 2r_p$,	$\frac{\sqrt{5} + 1}{2} \cdot \left[\frac{3\pi^2}{2} \right]^{\frac{1}{3}}$	3.972
Conical frustum, $R = r_p$, $r = \frac{R}{2}$, $h = 2r_p$	$5 + 3\sqrt{17} \left[\frac{3\pi^2}{2^8 \cdot 7} \right]^{\frac{1}{3}}$	4.423
Cube, $l = l_p$	6	6
Prism triangle, $l = l_p$, $h = l_p$	$\frac{6 + \sqrt{3}}{(2\sqrt{3})^{\frac{1}{3}}}$	5.114
Prism rectangle, $L = l_p$, $l = \frac{L}{2}$, $h = l_p$	$\frac{7}{2^{\frac{7}{3}}}$	5.04
Pyramid quadratae, $l = l_p$, $h = l_p$	$3^{\frac{1}{3}}(\sqrt{5} + 1)$	4.667
Regular pyramid (equilateral triangle base) $l = l_p$, $h = l_p$	$(\sqrt{39} + \sqrt{3}) \cdot \left(\frac{\sqrt{3}}{2^4} \right)^{1/3}$	3.802
Pyramid (hexagonal base), $l = l_p$, $h = l_p$	$\frac{5}{2^2} \cdot (\sqrt{7} + \sqrt{3})$	6.889
Truncated square pyramid, $L = l_p$, $l = \frac{L}{2}$, $h = l_p$	$\frac{3\sqrt{17} + 5}{4} \cdot \frac{12^{\frac{1}{3}}}{7}$	5.197

Fig. 1 and Fig. 2 present the critical acceleration values for particles of different shapes. The calculations were made for 973 K, and a value of contact angle for oxidised particles of SiC [15], Shen and Keene's relationships for surface tension of aluminium melt, Luca's equation for the density of aluminium liquid and a particle mass of $m_p = 1.344 \cdot 10^{-8}$ kg (equivalent to a spherical particle with a radius of 100 μm) [16, 17].

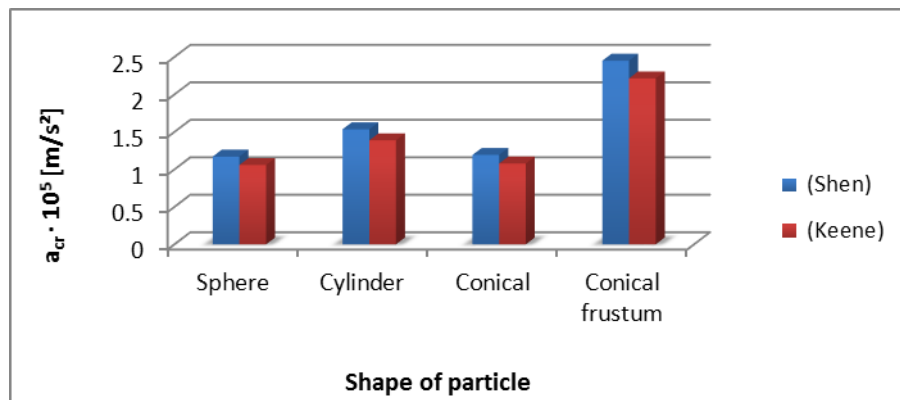


Fig. 1. Critical acceleration for round particles at 973K

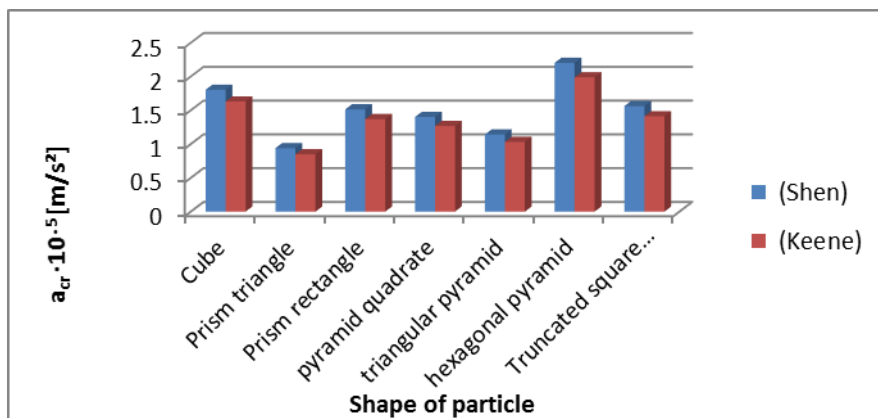


Fig. 2. Critical acceleration for polyhedral particles at 973K

From Fig. 1 and Fig. 2, the results show that triangle particles have minimum critical acceleration values compared to other shapes, but in spite of that, they are not sufficient for particle penetration.

The high values obtained by calculating the critical acceleration of particles show the need to apply a number of measures to improve the wetting conditions. The recommended measures, which include alloying of the melt with surface active elements, overheating of the metallic bath, and coating the particles or heat treatment of the complementary material, do not lead to a significant change in the system conditions.

This work presents a new method to obtain aluminium – silicon carbide particle composites by gravitational casting to improve the degree of incorporation between silicon carbide and melt aluminium.

3. Experimental conditions

Materials

Commercial aluminum was employed in this study; its chemical composition is listed in Table 2 and the major alloying element was silicon.

Table 2
Chemical composition of commercial Al alloy

Elements	Al	Fe	Cu	Mn	Mg	Si	Zn	Others
Wt.%	97.95	0.574	0.165	0.107	0.212	0.731	0.187	0.076

Sieves made from bonded textile fibers and SiC powders were used as raw materials. Four different sizes of SiC_p sieves: 40 mesh, 120 mesh, 180 mesh, and 220 mesh were chosen as the reinforcements.

Procedure

Sand molds were prepared and heated to 325°C to remove any moisture and reduce the temperature difference between the mold and the melt. The bonded SiC_p sieve covered both the base and inside wall of the mold, as shown in Fig. 3. The thicknesses of these sieves were 1.13 mm (for 40 mesh), 0.72 mm (120 mesh), 0.67 mm (180 mesh), 0.6 mm (220 mesh).

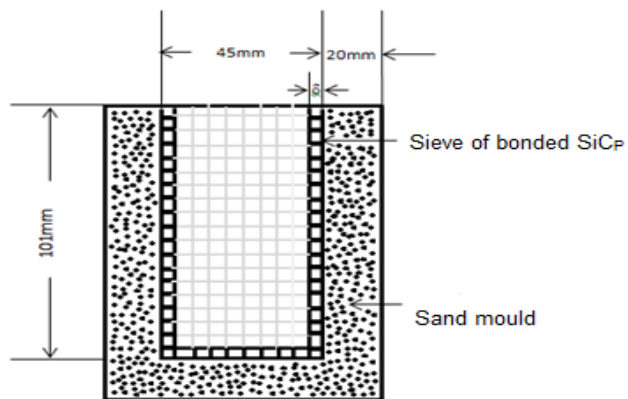


Fig. 3. Section of sand mold padded in SiCp

Al melt was prepared in a gas furnace, using a graphite crucible. Pouring aluminum melt in the mold was carried out at 900°C. After solidification, the samples were sectioned with an abrasive cutting machine into samples of 15 mm thickness from the middle, without causing any damage to the casting surface. Samples were ground with 120, 180, 320, 600, 800, 1000 grit papers respectively. Finally the polishing was finished on cloth using a diamond paste solution of 9

μm, 3 μm respectively, 2 min for each solution. The particle distribution and presence of SiC_p in the cast composites was identified by means of an optical microscope. The optical microscope is used for quality control applications and detailed examination of newly developed materials, metals, and chemicals. In this work, the instrument was used to study the microstructure of Al-SiC_p composite samples obtained by different methods, followed by image analysis.

4. Results and discussions

Fig. 4 (a-d) shows the pictures of the silicon carbide powder from sieves of different mesh sizes.

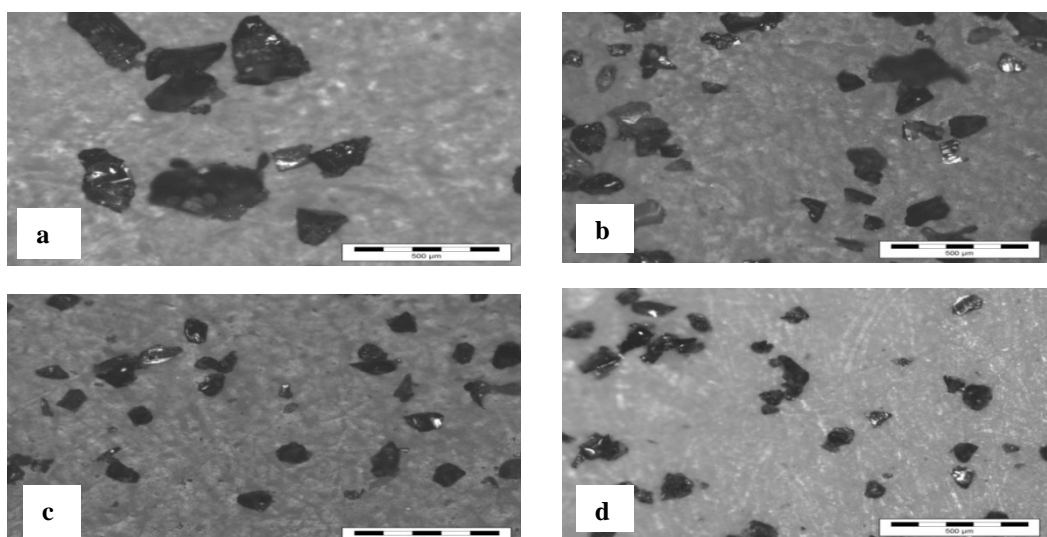


Fig. 4. Silicon carbide powder (a-particle size =0.587mm, b- particle size =0. 302mm, c- particle size =0. 276mm, d- particle size =0. 251mm).

Table 3 lists the size of SiC_p particles which were obtained from the optical microscope analysis.

Table 3

Analysis size of SiC _p				
Mesh no.of sieve	Mesh 40	Mesh 120	Mesh 180	Mesh 220
Particle size (mm)	0.587	0.302	0.276	0.251

The influence of particle shape on their behavior in the melt was investigated.

For the morphological characterization of SiC particles, different shape coefficients were measured; elongation ($EL=F/R$, F is the line connecting the two most distant points on the circumference, R - the equivalent rectangular shortest side); sphericity ($\Psi_w = d_v^2 / d_s^2$, d_v and d_s are the equivalent volume and surface diameter respectively; shape factor ($K_f = \text{thickness} / \sqrt{\text{length} \cdot \text{width}}$) [18-20].

The mean values of the shape coefficients of the particles were calculated (Fig. 4) and are listed in (Table 4).

Table 4
Mean values of shape coefficients for silicon carbide

Particle size (mm)	Elongation	Shape factor	Sphericity	Aspect ratio
0.587	1.287	0.554	0.429	1.4
0.302	1.585	0.573	0.45	1.54
0.276	1.59	0.601	0.461	1.553
0.251	1.644	0.603	0.479	1.58

When SiC_p was added into the aluminum melt, a number of modifications pertaining to its incorporation were observed, that will cause changes in its features, such as the mean shape coefficients' value, as a result of exposure to the phenomenon of erosion or the addition of impurities. The optical micrographs of aluminum composites reinforced with sieves of SiC_p are shown in Fig. 5.

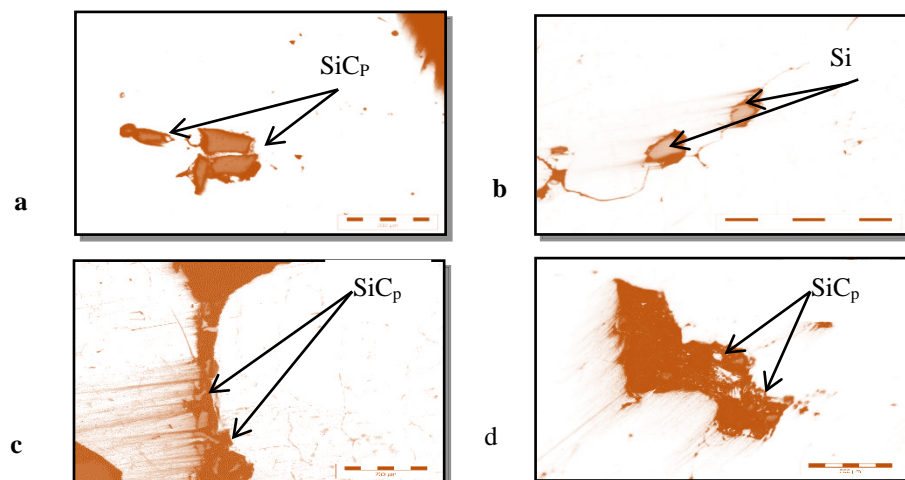


Fig. 5. Microstructure of Al-SiC_p composite for different sizes of powder sieves reinforced with aluminum: particle size a=0.587mm, b =0.302mm, c =0.276mm, d= 0.251mm).

Very irregular shapes and particle distribution was obtained with a clear tendency of inter granular distribution of the SiC particles. This may be caused by the low inoculation capacity of the SiC particles, depending of their inadequate surface properties or by the too low cooling rate of the melt during solidification.

Large size silicon carbide particles tend to segregate at the crystal grain boundaries. This segregation during solidification is harder to control, but can be limited by using a copper plate under the sand mold to increase the cooling rate and conduct crystallization. A superficial layer of Al-SiC_p composite improves the

tribological properties of moving and contacting components, such as the wear resistance in some automobile parts.

As seen in the results shown in Fig. 6, there seems to be an optimum size for SiC particles (0.276 mm) which assures a higher particle density on the sample section. This could be explained by the fact that the settlement of particles in the melt is already starting to occur when the melt is still in the mould. This is because the density of SiC_p is higher than that of the molten aluminum, which leads to settling or sedimentation of the particle reinforcements; therefore the higher sedimentation tendency of the bigger particles (0.587 mm, 0.302 mm) occurs when the alloy is in a liquid alloy state. At the same time, the smaller particles (0.251 mm) will tend to behave similarly to the bigger particles due to the agglomeration tendency, because

$$\Delta E_\sigma = \sigma_{lg} \cos \theta, \quad \theta > 0 \text{ and } \Delta E_\sigma < 0.$$

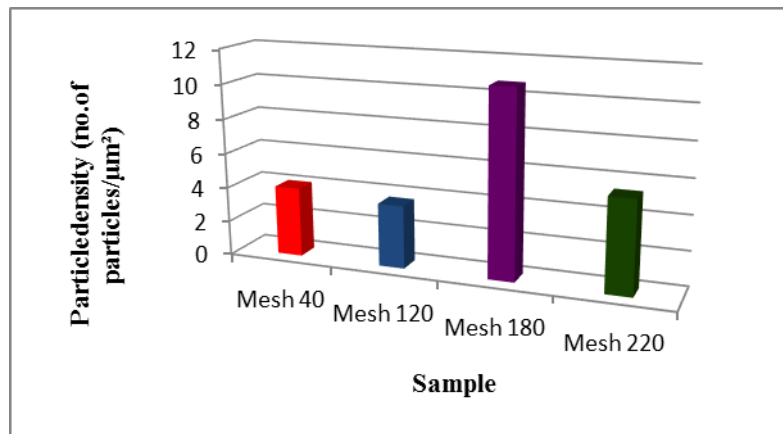


Fig. 6. Effect of particle size on silicon carbide particle density in the aluminum matrix (Mesh 40= particle size 0.587mm, Mesh 120= particle size 0.302mm, Mesh 180= particle size 0. 276mm, Mesh 20= particle size 0. 251mm)

Although there are significant difficulties in the quantification of particle shape, especially for irregular particles, the analysis of the several parameters proposed so far to describe both the SiC_p and Al-embedded SiC particles shapes has been generally accepted [21]. In this content, the results of shape coefficients' analysis, both of individual SiC particles (SiC powder) and Al-embedded SiC particles, are presented and compared in Fig.s 7- 10.

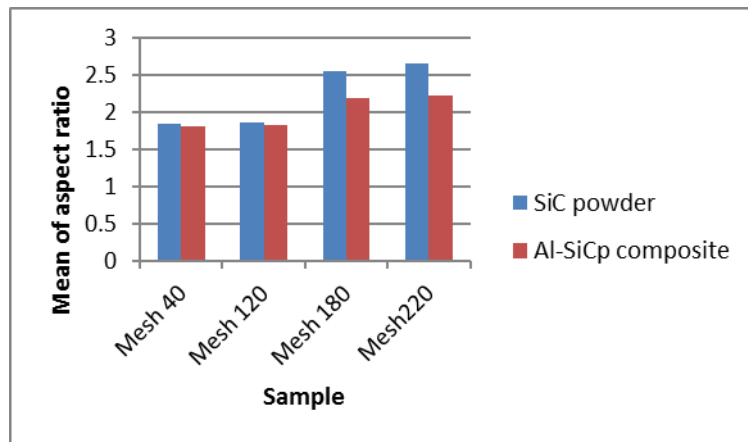


Fig. 7. Effect of particle size on mean silicon carbide aspect ratio in the aluminum matrix (Mesh 40= particle size 0.587mm, Mesh 120= particle size 0.302mm, Mesh 180= particle size 0. 276mm, Mesh 220= particle size 0. 251mm)

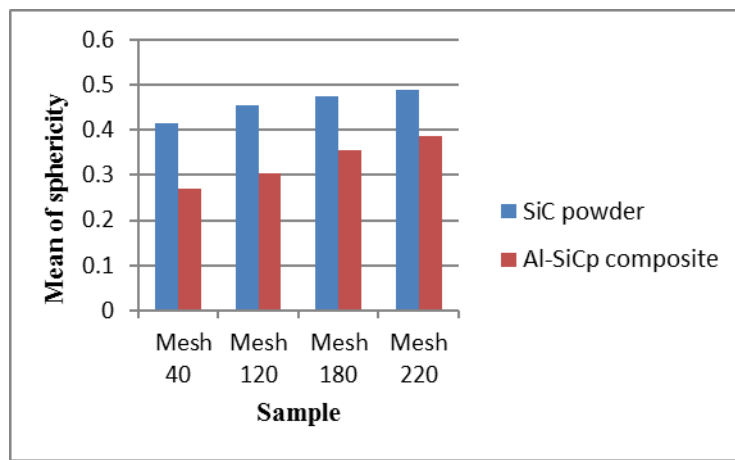


Fig. 8. Effect particle size on silicon carbide mean sphericity in the aluminum matrix (Mesh 40= particle size 0.587mm, Mesh 120= particle size 0.302mm, Mesh 180= particle size 0. 276mm, Mesh 220= particle size 0. 251mm)

As can be seen from Figs. 7-10, the values of SiC particle shape coefficients are constantly higher than the similar values for Al-embedded SiC particles, with a more significant difference for the mean of the sphericity factor (Fig. 8) [22]. This could be explained by a hollow which occurs around the free individual SiC particles, compared with the every sharp image of the embedded particles in the Al matrix.

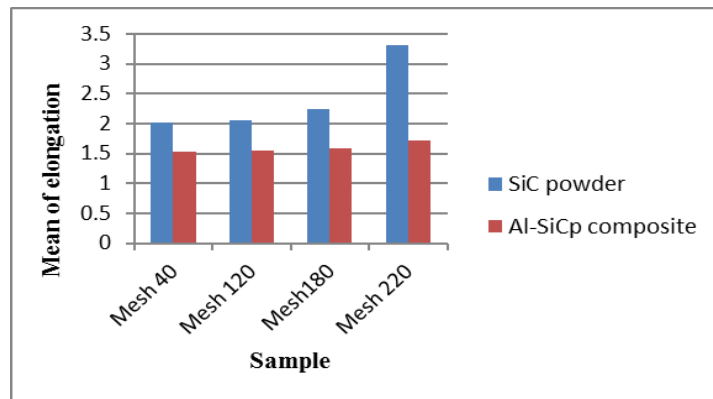


Fig. 9. Effect of particle size on silicon carbide mean elongation in the aluminum matrix (Mesh 40= particle size 0.587mm, Mesh 120= particle size 0.302mm, Mesh 180= particle size 0. 276mm, Mesh 220= particle size 0. 251mm)

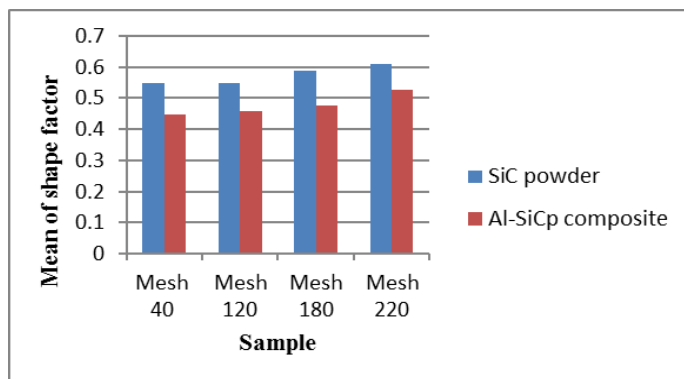
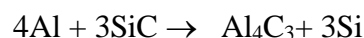


Fig. 10. Effect of particle size on silicon carbide mean shape factor in the aluminum matrix (Mesh 40= particle size 0.587mm, Mesh 120= particle size 0.302mm, Mesh 180= particle size 0. 276mm, Mesh 220= particle size 0. 251mm)

It was found that the elongation and aspect ratio of SiC_p were much higher than for Al-embedded SiC_p ; this may explained by a chemical reaction possibly occurring between the SiC particles and the melt aluminum alloy that forms another compound which remains in the melt, such:



The continuous reaction layer of Al_4C_3 occurred at 900°C between the melt aluminum and the silicon carbide [23]. The Al_4C_3 forms at the interface, while the Si dissolves in the Al matrix and causes a reduction in the shape coefficients' values.

5. Conclusions

A number of important conclusions may be drawn, as follows:

- Particle shape was an important parameter affecting the volumetric coefficient, and thus having an effect on the critical acceleration at different percentages (critical acceleration of conical frustum particle 62% higher than that of the prism triangle particle).

Due to the high acceleration values necessary for SiC_p to penetrate into the melt aluminum, a new method (sieves made from bonded SiC_p textile fibers) was used.

- There seems to exist an optimum SiC particle size (0. 276mm) which promotes a higher particle density on the cast sample section (10.7 no. of particle/μm²).
- Sphericity, elongation, shape factor and aspect ratio for SiC_p were higher than for the Al-SiC_p composite, due to the chemical reaction which took place between the SiC_p surface and aluminum. In addition, a number of defects, such as a hollow, led to a reduction in shape factors for Al-SiC_p.
- The segregation of silicon carbide particles must be slowed by high-speed solidification to improve the incorporation of the particles and the melt aluminum alloy.

R E F E R E N C E S

- [1]. *J.E. Schoutens and K. Tempo*, Introduction to Metal Matrix Composite Materials, DOD metal matrix composite information analysis center, 1982.
- [2]. *D. J. Lloyd*, Particle reinforced aluminium and magnesium matrix composites, International Materials Reviews, **vol. 39**, no.1, 1994.
- [3]. *K.K. Chawla*, "Composite Materials ", Springer-Verlag, New York, 1987.
- [4]. *C. Rado, S. Kalogeropoulou, N. Eustathopoulos*, Wetting and bonding of Ni-Si alloys on silicon carbide, *Acta Mater.* **47 (2)**, 1999, pp.461–473.
- [5]. *M. Singla, D. Deepak Dwivedi, L. Singh, and V. Chawla*, "Development of aluminium based silicon carbide particulate metal matrix composites", in *Journal of Minerals and Materials Characterization and Engineering*, **vol.8**, no.6, June 2009, pp. 455–467.
- [6]. www.NSM Archives-silicon carbide.
- [7]. *S. Balasivanandha Prabu, L. Karunamoorthy, S. Kathiresan, B. Mohan*, "Influence of stirring speed and stirring time on distribution of particles in cast metal matrix composite", in *Journal of Materials Processing Technology*, **vol. 171**, no. 2, January 2006, pp. 268-273.
- [8]. *R Mahadevan and R Gopal*, Selectively reinforced squeeze cast pistons, 68th WFC - World Foundry Congress 7th - 10th February, 2008, pp. 379-384.
- [9]. *P.Subramanya Reddy, R.Kesavan*, Investigation of Mechanical Properties of Aluminium Metal Matrix Composite (Al₂O₃ - SiC), *International Journal of Advanced Research in Science, Engineering and Technology*. **vol. 2**, Issue 10 , ISSN: 2350-0328, October 2015.
- [10]. *M. Dave and K. Kothari*, Composite Material-Aluminium Silicon Alloy: A Review, *Paripex-Indian Journal of research*, 2 (3), pp.148-150, 2013.

- [11]. *RAJAN, T. P. D., PILLAI, R. M., PAI, B. C.* Review – Reinforcement coatings and interfaces in aluminium metal matrix composites, *Journal of Materials Science* **33**, 1998, pp. 3491-3503.
- [12]. *UREÑA, A., ESCALERA, M.D., RODRIGO, P., BALDONEDO, J.L., GIL, L.* Active coatings for SiC particles to reduce the degradation by liquid aluminium during processing of aluminium matrix composites: study of interfacial reactions, *Journal of Microscopy*, **vol. 201**, pt. 2, February 2001, pp. 121-136.
- [13]. *A.S. Kacar, F. Rana, D.M. Ștefănescu*, Kinetics of gas-to-liquid transfer of particles in metal matrix composites, *Mat. Sc. Eng. A* **135**, 1991, pp. 95-100.
- [14]. *F. Dellanay, L. Froyen, A. Deruyterre*, Review. The wetting of solids by molten metal and its relation to the preparation of metal–matrix composites, *J. Mat. Sc.* **22** (1987) 1-16.
- [15]. *V. Laurent, D. Chatain, N. Eustathopoulos*, Wettability of SiC by aluminium and Al-Si alloys,
- [16]. *P. Shen, H. Fujii, T. Matsumoto, K. Nogi*, Influence of substrate crystallographic orientation on the wettability and adhesion of α -Al₂O₃ single crystals by liquid Al and Cu, *J. Mat. Sc.* **40** (2005).
- [17]. *B.J. Keene*, Review of data of surface tension of pure metals, *Intern. Mat. Rev.* **38/4** (1993) 157-192.
- [18]. *Fatima M. Barreiros Paulo J. Ferreira, M. Margarida Figueiredo*, calculating shape factors from particle sizing data, part. Part. Syst. Charact. **13**, 1996, pp.368-373.
- [19]. *Kuo, C-Y., and Feeman, R. B.*, Image analysis evaluation of aggregates for asphalt concrete mixture, transportation research record, No. 1615, TRB, NATIONAL REASEARCH COUNCIL, Washington, D. C., 1998, PP. 65-71.
- [20]. *Moustafa Saad, Abdelkrim Sadoudi, Eric Rondet, Bernard Cuq*, morphological characterization of wheat powders, how to characterize the shape of particles?, *Journal of food engineering* **102**, 2011, pp.293-301.
- [21]. *P. J. Lioyd*: The characterization of particle shape, in *P. J. Lioyd* (ed.): *Particle size analysis* 1988. Wiley, Chichester 1988.
- [22]. *J. M. Alexander, D. M. Bell, D. Imre, P. D. Kleiber, V. H. Grassian & A. Zelenyuk*, Measurement of size-dependent dynamic shape factors of quartz particles in two flow regimes, *Aerosol Science and Technology*, **50**, 2016, Issue 8, 870-879.
- [23]. *A. Urena, E. Martinez, P. Rodrigo, L. Gil*, Oxidation treatments for SiC particles used as reinforcement in aluminium matrix composites, *Composites Science and Technology* **64**, 2004, 1843-1854.